Turkish Journal of Electrical Engineering & Computer Sciences

http://journals.tubitak.gov.tr/elektrik/

Research Article

Turk J Elec Eng & Comp Sci
(2016) 24: 2429 – 2441

doi:10.3906/elk-1403-224

An efficient LOF-based long-range correlation filter for the restoration of salt and pepper impulse corrupted digital images

Justin VARGHESE[1,*], **Saudia SUBASH**[2], **Mohamed SAMIULLA KHAN**[3], **Krishnan NALLAPERUMAL**[2], **Bijoy BABU**[1], **Mohammed RAMADAN SAADI**[4]

[1]College of Computer Science, King Khalid University, Abha, Saudi Arabia
[2]Centre for Information Technology & Engineering, Manonmaniam Sundaranar University, India
[3]Department of Computer Science & Engineering, Manonmaniam Sundaranar University, India
[4]College of Science, South Valley University, Qena, Egypt

Received: 22.03.2014 • **Accepted/Published Online:** 14.08.2014 • **Final Version:** 15.04.2016

Abstract: The paper proposes an adaptive long-range correlation-based filter operator for the restoration of impulse corrupted digital images. The impulse detection scheme of the proposed algorithm incorporates the local outlier factor (LOF) to avoid the misclassification of uncorrupted pixels as noise. The restoration algorithm uses the local and remote neighborhood of the same size to find structural similarity among pixels for ensuring better replacement of detected impulses. The domain of the remote window is limited around the neighborhood of the impulsive pixel under concern for maintaining image details and thereby producing a high quality restored image. For replacing impulses, the filter uses a reference image and information about the corruption/purity status of the pixels in the image to determine the most correlated uncorrupted pixel from the remote neighborhood. Experimental results show that the proposed filter is capable of producing better results than the comparative filters in terms of subjective and objective metrics.

Key words: Adaptive filter, median filter, impulse noise, nonlocal filtering, image restoration

1. Introduction

Salt and pepper impulses affecting digital images are noises that occur when acquired through digital sensors or while transmitted through physical/electromagnetic media. These unwanted signals will affect the quality of the image by making true image pixels noisy. The corrupted image pixels take a very large value as a positive impulse or a very small value as a negative impulse and they respectively produce the visual salt and pepper-like effect in the corrupted image [1]. The median filter is one of the traditional impulse noise removal filters and is widely used due to its simplicity and detail preservation capability. A median filter replaces all the pixels of the image uniformly by the median of adjacent pixels from the predefined neighborhood without considering whether the pixel is corrupted or not [1]. With this background, many filters were proposed [1,2] to meet the contradictory requirements of noise reduction and signal preservation. Numerous transform-based algorithms [3–5] also evolved with different features to reduce noise while maintaining image perception quality. However, their performance was inefficient due to the large number of arithmetic calculations needed for obtaining the transformed image. Numerous switching schemes [6–14] also evolved by identifying the corrupted pixel positions and by replacing them with suitable values determined from detected uncorrupted pixels. Mu et al. [15] proposed

*Correspondence: justin_var@yahoo.com

a fast and efficient median filter (FEMF) by addressing the limitation of the adaptive switching median filter [10], but it failed to preserve structural details of the local neighborhood while restoring impulses. Shi et al. [16] proposed a sorted switching median filter by incorporating histogram-based impulse detection and trimmed median-based regularization to efficiently replace impulses, but it failed to avoid misclassification when the image is corrupted at lower impulse noise levels. Although these algorithms performed better, they could not meet the requirements of perfectly identifying the corrupted pixel positions and adequately replacing it with a suitable value. The algorithm proposed by Awad [17] used a direction-based approach where optimal direction is used as a reference for identifying corrupted pixels, but the algorithm is limited to perform better only at low noise levels. Jafar et al. [18] addressed the limitations of boundary discriminative noise detection (BDND) [19] by incorporating a clustering scheme to classify pixels by their corrupted/uncorrupted status. The LOF-based boundary discriminative noise detection filter (LOFBDND) proposed by Wang et al. [20] incorporated the LOF to quantify the distinctiveness of corrupted pixels. However, the algorithm failed to restore images corrupted at higher quantum of impulse levels since it set the correction window size to 3×3 and also by considering all pixels irrespective of them being corrupted or not to restore impulses.

Due to the detail preservation capability, many nonlocal correlation based algorithms were developed by focusing on the replacement of impulses by one of the uncorrupted remote pixels that best suits the image local conditions. The decision-based nonlocal mean (DNLM) filter [21] used a statistics-based classification scheme to detect corrupted pixels and the corrupted pixels are replaced with suitable values by considering reference image output along with nonlocal means. The algorithm proposed by Jie [22] used functional level evolution (FLE) to identify the remote pixel to replace the detected impulses, but the algorithm introduced impulsive patches in the restored image while restoring highly corrupted images. The long-range correlation (LRC) based filter [23] works with the stages of impulse detection and noise cancellation. The signal estimate for replacing impulses is obtained based on the mean square error measure between the nonimpulsive pixels of the local window and the remote window. However, the impulse correction scheme fails in efficiently replacing impulses at higher impulse noise ratios due to the difficulties in highly impulse corrupted environments where almost all pixels of the remote window and the window under consideration are corrupted. This increases the time complexity of the algorithm due to the search for neighborhoods with uncorrupted pixels. Moreover, it does not account for the homogeneity of pixels in the local window and the remote window while determining the signal restorer. Thus almost all filters in the literature could not simultaneously meet all the requirement of detection and correction of impulses.

In this paper we propose an adaptive local outlier-based long-range correlation filter for the restoration of salt and pepper impulse corrupted digital images by addressing the limitations of LRC, LOFBDND, and DNLM filters. The paper is organized in four sections. Section 2 provides the proposed impulse restoration filter. Experimental results and simulation analysis are given in Section 3. Conclusions are made finally in Section 4.

2. The proposed algorithm

The proposed algorithm incorporates the distinct phases of impulse detection and correction. The impulse detection algorithm is built in with the min–max and LOF criteria to efficiently identify impulsive positions and thereby to avoid the misclassification of uncorrupted pixels as noise and vice versa. The proposed filter is designed with the assumption that image pixels are smoothly varying and are separated by edges. The noise model considered by our algorithm is only salt and pepper impulse noise, which means 1) only a portion

of image pixels will be corrupted; 2) the corrupted pixel can take either a minimum or maximum value of the dynamic range [1]. The proposed restoration algorithm is incorporated with long-range-based correlation calculations to find the structural similarity for effectively replacing the detected impulses with the respective remote pixels that better suit the local image conditions. The proposed filtering scheme is explained in the following subsections.

2.1. The impulse detection stage

The impulse detection phase of the proposed filter aims at identifying the corrupted positions in a flag image, f, of same size, $M \times N$, as the given corrupted input image, X, where f_i and X_i, respectively, provide the flag and pixel value at position $i = (i_1, i_2)$. We denote the impulsive and nonimpulsive positions of the corrupted input image by setting the corresponding positions of the flag image, f, respectively as 1 and 0. As an initial step, we set all spatial positions of the flag image f to '1' by assuming that the entire image is corrupted, i.e.

$$f = \left\{ f_{i=(i_1,i_2)} = 1 / 1 \leq i_1 \leq M, 1 \leq i_2 \leq N \right\} \tag{1}$$

The traditional min–max check is utilized to perform the initial assessment of corrupted/uncorrupted status of each pixel. For each pixel at position $i = (i_1, i_2)$, we determine the minimum and maximum values of the image pixels defined by the impulse detection window $W_D \times W_D$ centered at position i to check the purity status of respective image pixel X_i. We generalize Ω_i^W to denote the set of pixel positions in the window $W \times W$ centered at position $i = (i_1, i_2)$ and is mathematically expressed as

$$\Omega_i^W = \{ j = (j_1, j_2) / i_1 - k \leq j_1 \leq i_1 + k, i_2 - k \leq j_2 \leq i_2 + k \} \tag{2}$$

Here $k = (W-1)/2$ and the purity status is recorded in the initial flag image, f^I, as

$$f_i^I = \begin{cases} 0 \text{ if } (X_i - m_1) > 0 \text{ and } (X_i - m_2) < 0 \\ 1 \text{ otherwise} \end{cases} \tag{3}$$

where

$$m_1 = \min \left\{ X_j / j \in \Omega_i^{W_D} \right\} \tag{4}$$

$$m_2 = \max \left\{ X_j / j \in \Omega_i^{W_D} \right\} \tag{5}$$

Here W_D is an odd integer not smaller than 3.

Once the initial assessment of the flag image is made, since there are chances of wrongly detecting uncorrupted pixels as noisy especially when the noise ratio is less, we refine the status of detected corrupted pixels by determining its LOF from the set of nearest uncorrupted pixels, S, defined by

$$S = \left\{ X_j / m_1 < X_j < m_2 \text{ and } j \in \Omega_i^{W_D} \right\} \tag{6}$$

The LOF of X_i over the set of uncorrupted pixels, S, provides how much X_i is isolated from the detected uncorrupted pixels. Note that this LOF calculation is possible only when there are sufficient pixels in the uncorrupted set, S. If the cardinality of S is greater than a predefined threshold, T_1, indicating sufficient

uncorrupted pixels in the set, S, to determine the outlier nature of X_i, we calculate LOF of X_i over the set of uncorrupted pixels, S. For any pixel p, the r-neighbor $LOF_r(p)$ is defined by

$$LOF_r(p) = \left(\frac{\sum_{B \in N_r(X_i)} lrd_r(B) \Big/ lrd_r(p)}{|N_r(p)|} \right), \tag{7}$$

where $lrd_r(p)$ is the local reachability density of p from its r-distance pixels and $|N_r(p)|$ is the cardinality of set of pixels in r-distance neighborhood of p. Here the distance refers to the pixel intensity difference. Further, the formulation and definitions of LOF can be found from [24]. If $LOF_r(X_i)$ is near to 1, it is a good indication that X_i shows good correlation with its uncorrupted r-distance neighboring pixels from S and hence it need to be declared uncorrupted. In our algorithm, we not only use $LOF_r(X_i)$ but also the 1-distance neighbor $LOF_r(N_1(X_i))$ (the LOF of the closest uncorrupted pixel from X_i) to better ensure the purity status of X_i. We define the final refined flag image f_i as

$$f_i = \begin{cases} 0 \text{ if } (|LOF_r(N_1(X_i)) - LOF_r(X_i)| \leq T_2) \text{ and } f_i^I = 1 \\ f_i^I \text{ otherwise} \end{cases} \tag{8}$$

Here T_2 is the threshold used for fixing the LOF tolerance level for changing the corrupted status of the pixels. Since we incorporated a two-way LOF-based comparison to refine the detected corrupted pixels from the first phase of impulse detection using traditional min–max check, many uncorrupted edge pixels that are similar to the noise will escape from being misclassified as impulse.

2.2. The impulse correction stage

The proposed filter incorporates flag and reference images in the process of image restoration where the flag image f provides the corruption/purity status of pixels, whereas the reference image U^{ref} is the filtered output of another filter using the same flag image. We use the impulse correction phase of one of our previously published work, adaptive switching median filter (ASMF) [10] to construct the reference image, U^{ref}, by using the flag image of this proposed impulse detection algorithm and it is utilized for the efficient replacement of detected impulses by the proposed correction algorithm. The proposed algorithm makes use of local and remote windows of same size, $W_1 \times W_1$, to identify the better restorer of the search window from the neighborhood of the corrupted pixel defined by the mask, $W_2 \times W_2$. Note that $W_1 < W_2$ and $W_1 = 2k_1 + 1$ and $W_2 = 2k_2 + 1$. The proposed restoration algorithm is described in the following steps:

Step 1: If the flag value f_i of position, $i = (i_1, i_2)$ of the pixel U_i is '0', it is retained in the restored image, V_i, since U_i is an uncorrupted pixel. Thus,

$$V_i = U_i \tag{9}$$

Now the algorithm is continued from Step: 5.

Step 2: Otherwise if the flag value, f_i of the pixel U_i is '1', indicating an impulsive position, we use two windows of sizes $W_1 \times W_1$ and $W_2 \times W_2$ such that $\Omega_i^{W_1} \subset \Omega_i^{W_2}$. For each corrupted pixel, in order to ensure the structure preservation in the restored image V, we find the remote uncorrupted pixel U_j such that $j \in \Omega_i^{W_2}$

that best suits the local image conditions of the neighborhood of U_i. This U_j is found in R by considering the corresponding neighboring pixels in the reference image, U^{ref}, defined by the set of positions, $\Omega_j^{W_1}$, that produces the least weighted mean square error with the neighboring pixels defined by $\Omega_i^{W_1}$ of U_i^{ref} as

$$R = \arg\min_{U_j} \left\{ \frac{\sum_{l_1=-k_1}^{k_1} \sum_{l_2=-k_1}^{k_1} Wt_{ijl_1l_2} \times \left(U^{ref}_{i_1+l_1,i_2+l_2} - U^{ref}_{j_1+l_1,j_2+l_2} \right)^2}{\sum_{l_1=-k_1}^{k_1} \sum_{l_2=-k_1}^{k_1} Wt_{ijl_1l_2}} \times d_{i,j,l_1,l_2} \right\}_{j=(j_1,j_2)\in\Omega_i^{W_2}\setminus(i_1,i_2)} \tag{10}$$

where '$\setminus$' is the set difference operator and

$$Wt_{i,j,l_1,l_2} = \left(1 - \left(\frac{(f_{i_1+l_1,i_2+l_2} + f_{j_1+l_1,j_2+l_2})}{3}\right)\right) \tag{11}$$

The Wt_{i,j,l_1,l_2} provides the weight for each squared pixel difference calculation and d_{i,j,l_1,l_2} is the distance between the positions (i_1+l_1, i_2+l_2) and (j_1+l_1, j_2+l_2). We have assigned minimum weight when both the local and remote neighboring pixels from the reference image are corrupted.

Step 3: Here if $|R - U_i| \leq T_3$, it indicates that there is a strong correlation between the center pixel U_i with that of the found restorer R and hence we maintain the center pixel as in (9). Here T_3 is a threshold used for checking the correlation of the restoring value, R, with the central pixel, U_i.

Step 4: Otherwise if $|R - U_i| > T_3$, we replace the center pixel U_i by R as

$$V_i = R \tag{12}$$

Step 5: Move to the next pixel and process it from step 1.

Unlike other algorithms [22,23], since the proposed algorithm makes use of the reference image while replacing impulses, we always get a valid restorer in the first iteration itself and thereby it reduces the computational complexity to a large extent. Moreover, the additional importance in terms of weights given to the uncorrupted pixels while determining the weighted squared error helps the algorithm to identify the remote pixel that better suits the local image structural properties while replacing impulses.

3. The experimental results and analysis

In this section, we compare the proposed algorithm in terms of efficiency and detail preservation capability with other algorithms including simple median filter [1], center weighted median filter (CWMF) [2], rank ordered mean (ROM) Filter [6], morphological median filter (MMF) [7], progressive switching median filter (PSMF) [8], pixel restoring median filter (PRMF) [9], noise adaptive fuzzy switching median filter (NAFSMF) [11], fuzzy mean linear aliasing window kernel filter (FMLAWKF) [12], pixel correlation based impulse filter (PCIF) [13], switching-based adaptive weighted mean filter (SAWMF) [14], boundary discriminative noise detection filter (BDNDF) [19], local outlier factor based boundary discriminative noise detection filter (LOFBDND) [20], decision-based non-local means filter (DNLMF) [21], long range correlation filter (LRCF) [23], adaptive fuzzy based switching weighted average (AFSWA) filter [25], and rank ordered adaptive median filter (RAMF) [26]. The various test images used for analyzing the subjective and objective performance of the proposed algorithm

include Lena, Boats, Cameraman, Bridge, Barbara, and Baboon. The 8-bit Lena and Boats images of size 512 $\times$ 512 are used in this paper for experimental comparisons.

The objective comparison is made with peak signal to noise ratio (PSNR), the mean absolute error (MAE), miss-detection (MD), and false alarm (FA). The formulations for PSNR and MAE are as defined in AFSWA. MD provides the total number of misclassifications of impulses as signals whereas the FA provides the total number of misclassifications of signals as impulses by the impulse detection algorithms. A better impulse detection algorithm should produce fewer MDs and FAs by clearly isolating impulses from signals.

We use visual analysis of the restored outputs, percentage of not detected edges, $\xi_1(\%)$, and the percentage of wrongly detected edges, $\xi_2(\%)$, to compare the subjective performance of the proposed algorithm over other prominent filters. The metric ξ_1 is the percentage of ratio of edge pixels present in the edge image from the impulse-free image but not present in the edge image of the impulse filter's output to the total number of edge pixels present in the noise-free image, while ξ_2 is the percentage of edges present in the edge image of the restored output but not present in the edge image of the impulse-free image to the total number of nonedge pixels present in the restored image. Figures 1 and 2 make the visual comparison of the outputs produced by SAWMF, PCIF, NAFSMF, FMLAWKF, DNLMF, AFSWAF, and the proposed algorithm for impulse noise ratios 10% and 50%, respectively, on the Lena image. Restored outputs produced by FMLAWKF, DNLMF, AFSWAF, and the proposed algorithm from the Lena image corrupted with 90% noise are shown in Figure 3. From visual analysis, it is very clear that the restored outputs produced by the proposed algorithm are better than those of the other competitive algorithms.

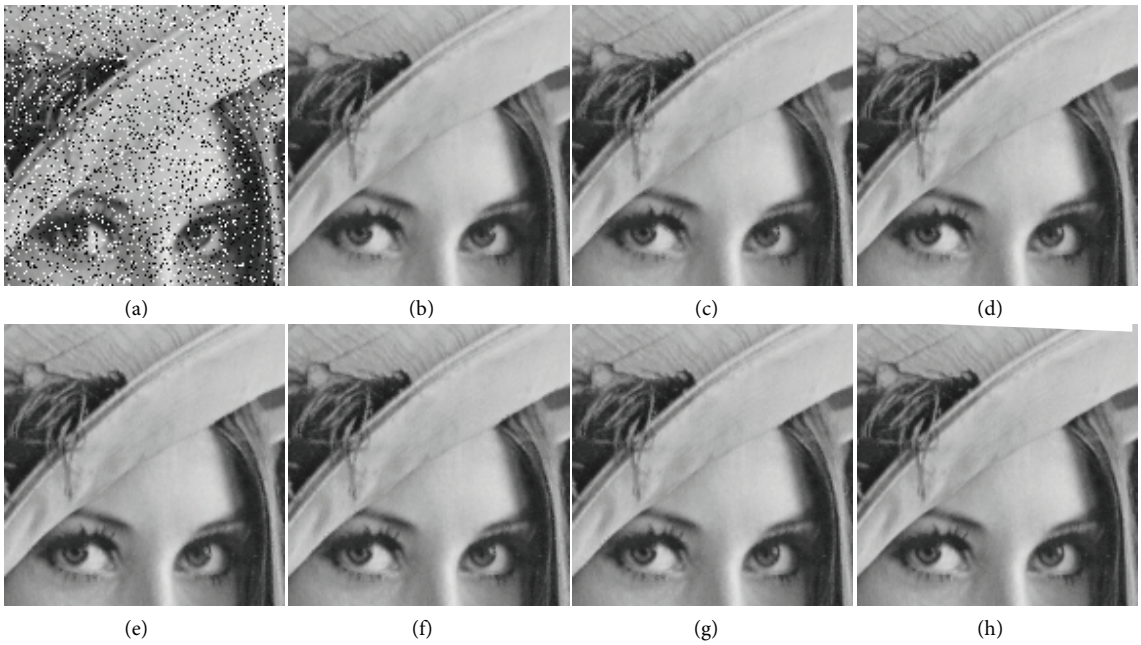

Figure 1. Outputs of different methods in restoring the Lena image corrupted at 10% noise level: (a) corrupted image, (b) SAWMF, (c) PCIF, (d) NAFSM, (e) FMLAWK, (f) DNLN, (g) AFSWA, and (h) the proposed filter.

Figure 4 provides a visual comparison of the edge distortions in the restored outputs produced by SAWMF, PCIF, NAFSMF, FMLAWKF, DNLMF, AFSWAF, and the proposed algorithm on the Lena image corrupted with 10% noise. The correctly retained edges in the restored image the same as in the case of the noise-free

image is represented by blue color. The edges present in the edge detected image of the impulse-free image but not present in the edge detected image of the restored output by different filters are indicated by red color. In addition, the edges that are present in the edge image of the restored output but are not present in the edge image of the impulse-free image are indicated by blue color pixels. It is to be noted that the edge preservation capability of the proposed algorithm is better when compared to other promising algorithms in the literature as can be verified from Figure 4.

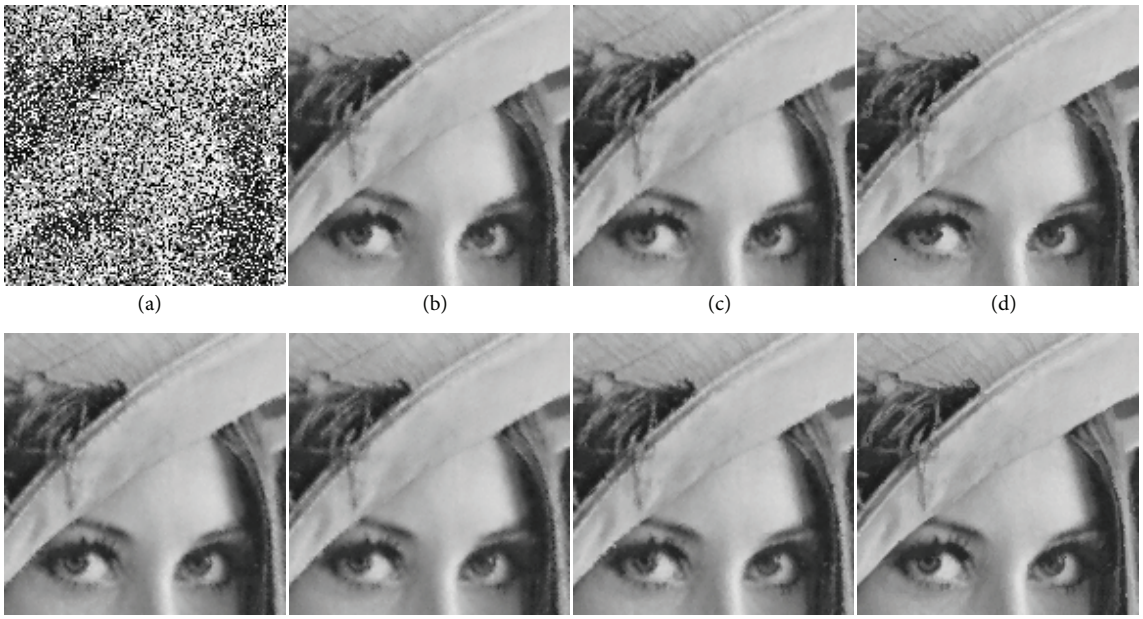

Figure 2. Outputs of different methods in restoring the Lena image corrupted at 10% noise level: (a) corrupted image, (b) SAWMF, (c) PCIF, (d) NAFSM, (e) FMLAWK, (f) DNLN, (g) AFSWA, and (h) the proposed filter.

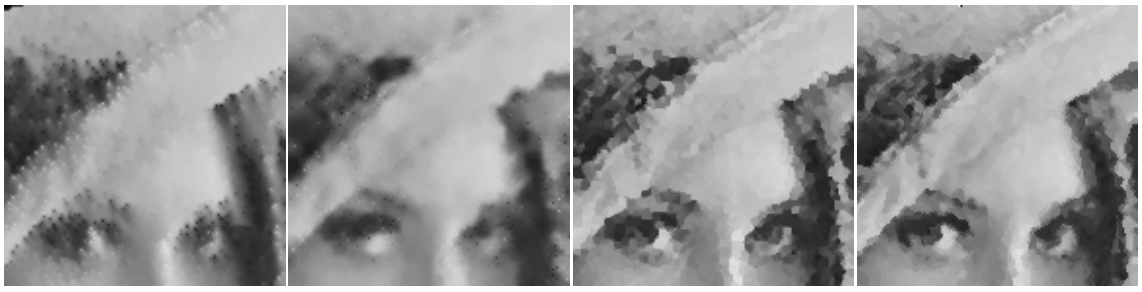

Figure 3. Outputs of different methods in restoring the Lena image corrupted at 90% noise level: (a) FMLAWK, (b) DNLN, (c) AFSWA, and (d) the proposed filter.

Tables 1–3 respectively show the objective analysis of PSNR, MAE, ξ_1, ξ_2, MD, and FAs on the restored images produced by different filters from the Lena image corrupted by 10%, 50%, and 90%. The analysis on PSNR, MAE, ξ_1, ξ_2, MD, and FAs on the restored images produced by different filters from the Boats image corrupted by 10%, 50%, and 90% are respectively shown in Tables 4–6. From Tables 1–6, it is very clear that the objective performance of the proposed algorithm is better than that of the other comparative filters.

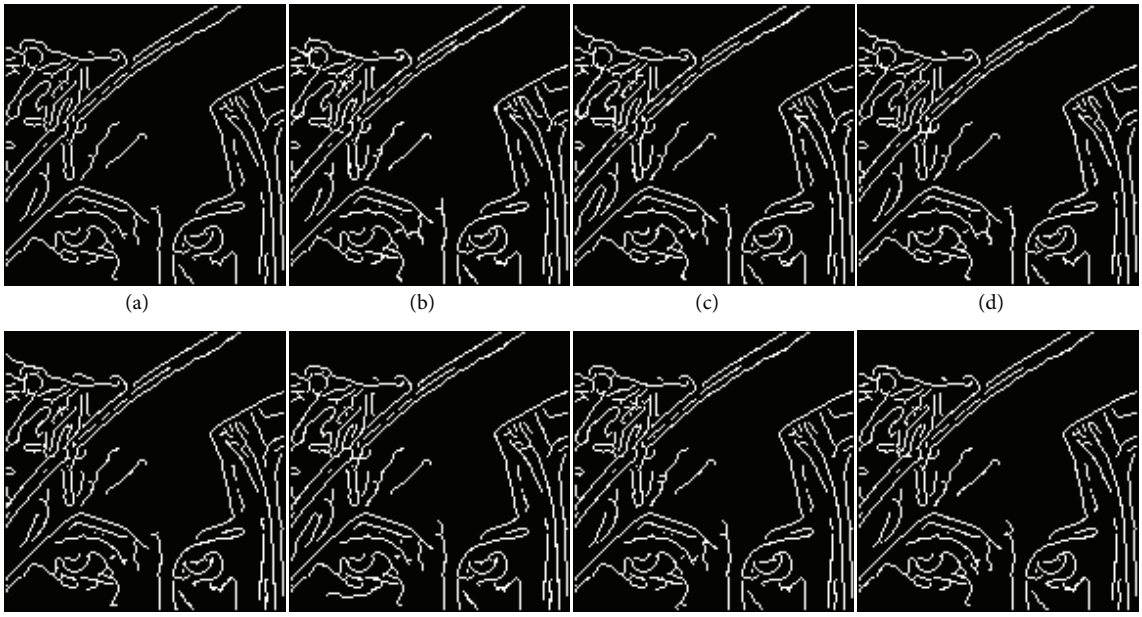

Figure 4. Edge images by Canny method with correctly detected (green), not detected (red) and wrongly detected (blue) edge positions of restored outputs of different filters from the Lena image corrupted with 10% noise: (a) uncorrupted image, (b) SAWMF, (c) PCIF, (d) NAFSM, (e) FMLAWK, (f) DNLN, (g) AFSWA, and (h) the proposed filter.

Table 1. Objective metrics produced by different filters for Lena corrupted by 10% impulse noise.

Filters	PSNR	MAE	ξ_1	ξ_2	MD	FA
MMF 3×3	30.252	4.269	4.275	3.100	0	217,765
ROM 3×3	32.634	3.183	2.358	1.704	3	206,269
CWMF 3×3	33.577	1.749	1.609	1.413	144	93,306
Median 3×3	33.712	2.760	2.144	1.425	4	160,492
PSMF	33.961	0.794	0.936	1.320	11	76
RAMF	38.092	0.964	1.079	0.865	0	30,224
SAWMF	38.676	0.927	1.032	0.802	32	57
LRCF	38.799	0.493	0.839	0.674	47	58
PCIF	38.930	0.706	0.939	0.764	43	31
LOFBDND	40.784	0.394	0.676	0.656	123	32
BDND	41.152	0.348	0.619	0.564	0	3
NAFSM	41.860	0.432	0.730	0.656	0	15
FMLAWK	42.331	0.380	0.608	0.547	0	11
DNLM	42.405	0.377	0.633	0.558	0	10
AFSWA	42.413	0.377	0.595	0.528	1	0
Proposed	43.392	0.372	0.527	0.534	0	1

Table 2. Objective metrics produced by different filters for Lena corrupted by 50% impulse noise.

Filters	PSNR	MAE	ξ_1	ξ_2	MD	FA
MMF 5×5	27.545	5.718	4.289	5.099	0	124,657
ROM 7×7	26.934	6.001	4.532	3.614	12	118,324
CWMF 7×7	27.139	5.573	4.305	3.500	81	96,078
Median 7×7	26.973	5.986	4.565	3.566	17	110,693
PSMF	28.335	3.376	3.369	2.931	29	4061
RAMF	29.820	3.144	2.987	2.936	0	3316
SAWMF	33.155	2.325	2.433	1.953	107	28
LRCF	28.135	3.666	3.011	2.637	105	16
PCIF	33.905	2.154	2.098	1.801	45	53
LOFBDND	30.110	3.202	3.165	2.042	83	10
BDND	29.995	3.001	2.747	2.822	0	114
NAFSM	33.01	2.371	2.195	1.996	0	1
FMLAWK	33.346	2.288	2.315	1.852	0	3
DNLM	33.724	2.205	2.193	1.608	0	4
AFSWA	33.597	2.184	2.055	1.713	0	0
Proposed	34.315	2.103	1.899	1.710	0	0

Table 3. Objective metrics produced by different filters for Lena corrupted by 90% impulse noise.

Filters	PSNR	MAE	ξ_1	ξ_2	MD	FA
MMF 9×9	12.330	49.871	6.384	8.499	4045	25,539
ROM 9×9	9.892	54.018	5.992	12.315	44159	25,168
CWMF 9×9	9.410	56.000	6.028	12.640	69175	18,762
Median 9×9	9.647	53.408	5.965	12.310	50017	22,894
PSMF	12.360	31.884	6.379	5.143	4224	12,800
RAMF	21.402	10.501	6.361	7.238	386	5
SAWMF	24.424	7.410	5.605	5.037	58	86
LRCF	7.356	85.775	6.203	10.473	536	763
PCIF	26.191	6.797	5.305	4.661	43	57
LOFBDND	23.110	7.202	5.765	5.042	320	10
BDND	16.181	13.354	6.182	5.064	102	539
NAFSM	24.600	7.265	5.213	5.944	549	9
FMLAWK	23.740	8.835	5.503	5.178	0	5
DNLM	26.636	6.309	5.457	4.563	0	3
AFSWA	26.210	6.332	4.956	5.092	0	0
Proposed	26.280	6.185	4.958	4.537	0	0

Table 4. Objective metrics produced by different filters for Boats corrupted by 10% impulse noise.

Filters	PSNR	MAE	ξ_1	ξ_2	MD	FA
MMF 3×3	27.236	6.245	5.819	3.743	0	224,119
ROM 3×3	29.257	4.989	3.410	2.587	2	217,722
CWMF 3×3	30.572	2.895	2.682	2.113	166	107,691
Median 3×3	29.764	4.517	3.385	2.242	11	175,824
PSMF	32.796	0.986	1.459	1.263	35	677
RAMF	33.875	1.563	1.679	1.396	0	29,551
SAWMF	34.104	1.538	1.607	0.805	131	102
LRCF	31.476	1.129	1.670	1.594	98	107
PCIF	34.129	1.254	1.453	1.531	94	73
LOFBDND	37.603	0.616	1.033	1.065	965	114
BDND	36.565	0.636	1.024	0.945	0	8
NAFSM	37.850	0.694	1.068	0.936	0	7
FMLAWK	37.145	0.785	1.173	1.119	0	8
DNLM	38.409	0.606	0.929	0.865	0	119
AFSWA	38.258	0.590	0.986	0.915	0	0
Proposed	39.643	0.497	0.909	0.881	0	5

Table 5. Objective metrics produced by different filters for Boats corrupted by 50% impulse noise.

Filters	PSNR	MAE	ξ_1	ξ_2	MD	FA
MMF 5×5	24.547	8.599	7.925	4.511	0	126,940
ROM 7×7	23.832	9.200	8.457	5.035	14	122,900
CWMF 7×7	24.028	8.576	8.215	4.525	81	102,932
Median 7×7	23.767	9.187	8.410	5.118	20	116,372
PSMF	24.127	6.167	6.119	4.340	72	8241
RAMF	27.015	4.639	4.543	3.848	0	3319
SAWMF	29.307	3.696	3.799	1.957	32	341
LRCF	24.100	6.473	5.313	4.758	230	589
PCIF	30.231	3.361	3.099	2.814	17	34
LOFBDND	26.020	5.280	4.998	5.658	756	106
BDND	26.433	4.706	4.657	3.692	0	264
NAFSM	29.161	3.719	3.452	3.004	0	0
FMLAWK	29.457	3.850	3.821	3.096	0	3
DNLM	29.980	3.475	3.402	2.632	0	5
AFSWA	30.433	3.231	3.148	2.584	0	0
Proposed	30.606	3.193	3.046	4.470	0	0

Table 6. Objective metrics produced by different filters for Boats corrupted by 90% impulse noise.

Filters	PSNR	MAE	ξ_1	ξ_2	MD	FA
MMF 9×9	12.450	49.434	9.562	8.1680	2986	25,878
ROM 9×9	9.707	57.019	9.026	12.413	43858	25,582
CWMF 9×9	9.404	57.808	9.022	11.969	68261	19,365
Median 9×9	9.462	57.192	8.957	12.380	51471	23,569
PSMF	12.101	34.838	9.268	4.837	665	14,878
RAMF	20.074	13.601	8.784	9.067	196	5
SAWMF	22.451	10.420	8.687	5.237	62	17
LRCF	7.169	90.369	9.268	9.798	636	914
PCIF	23.230	9.6190	8.137	5.831	21	28
LOFBDND	20.110	17.202	8.765	7.042	320	10
BDND	16.690	18.861	9.330	7.419	0	661
NAFSM	22.240	10.460	7.915	7.347	568	1
FMLAWK	20.635	14.578	8.786	6.724	0	2
DNLM	23.851	9.293	8.410	6.862	0	1
AFSWA	23.401	9.332	7.156	6.491	0	0
Proposed	24.437	9.267	7.100	6.238	0	0

The thresholds T_1, T_2, and T_3 are used for fine tuning the performance of the proposed algorithm. T_1 decides the minimum number of uncorrupted pixels needed in the impulse free set, S, to perform LOF calculations to refine the corrupted status of pixels. T_3 decides the tolerance level to omit a pixel from replacing it with a restoration value. We take a very small value in the range [0, 5] for set T_3. Among all thresholds, T_2 plays an important role that affects the overall performance of the proposed filter and its behavior is explained through the following cases as can be verified from Table 7.

Table 7. PSNR obtained from the Lena image for different T_2 values against various impulse noise levels.

Noise ratio	PSNR for different T_2values								
	$T_2 = 0.5$	$T_2 = 1.0$	$T_2 = 1.5$	$T_2 = 2.0$	$T_2 = 2.5$	$T_2 = 3$	$T_2 = 3.5$	$T_2 = 4.0$	$T_2 = 4.5$
2	48.194	48.619	48.979	49.235	49.535	49.652	49.709	49.840	49.900
4	46.885	47.002	47.093	47.208	47.306	47.325	47.334	47.372	47.372
6	45.492	45.536	45.551	45.576	45.594	45.606	45.610	45.627	45.632
8	44.544	44.559	44.565	44.577	44.583	44.586	44.586	44.589	44.589
10	43.366	43.379	43.381	43.386	43.389	43.390	43.390	43.391	43.392
12	42.427	42.429	42.430	42.430	42.432	42.432	42.432	42.432	42.432
14	41.616	41.616	41.617	41.617	41.618	41.618	41.619	41.619	41.619
16	41.045	41.045	41.045	41.046	41.046	41.046	41.046	41.046	41.046
18	40.427	40.427	40.427	40.427	40.428	40.428	40.428	40.428	40.428
20	39.964	39.964	39.964	39.964	39.964	39.964	39.964	39.964	39.964

Case 1: If the image is corrupted with low noise levels, many uncorrupted pixels in the window will be misclassified as impulses by the min–max check in (3); all of them will participate in the 2-way LOF based refinement. The threshold T_2 in this case should be large enough to avoid misclassification of uncorrupted pixels as noisy.

Case 2: If the image is corrupted with a higher quantum of impulse noise, much fewer uncorrupted pixels in the window will be misclassified as impulses by the min–max check; all of them will participate in the 2-way LOF-based refinement. Although the threshold T_2 in this case is less obvious, it should be small enough to avoid misclassification of corrupted pixels as uncorrupted. By empirical analysis on different images, we formulated T_2 as

$$T_2 = (1 - NR) \times a_1 \tag{13}$$

Here a_1 is a constant and the local noise ratio NR is determined by

$$NR = \frac{(1 - |S|)}{W^D \times W^D} \tag{14}$$

Here S is the set of uncorrupted pixels from (6) and $||$ denotes its cardinality. The window sizes W_D, W_1, and W_2 are respectively set to 7, 7, and 3 for better performance of the algorithm. For the other algorithms, we used the parameters as suggested in the respective papers.

4. Conclusion

The proposed adaptive long-range correlation-based filter operator for the restoration of impulse corrupted digital images incorporates the LOF in its detection scheme to avoid the misclassification of uncorrupted pixels as noise. Since the filter uses the reference image and information about the corruption/purity status of the pixels in the image to determine the most correlated uncorrupted pixel from the remote limited neighborhood around the pixel under concern, the errors while replacing impulses are reduced. Experimental results showed that the outputs produced by the proposed filter are better than the results of other prominent filters in terms of subjective and objective metrics.

References

[1] Gonzalez RC, Woods RE. Digital Image Processing. 3rd ed. Upper Saddle River, NJ, USA: Prentice Hall, 2008.

[2] Ko SJ, Lee YH. Center weighted median filters and their applications to image enhancement. IEEE T Circuits-I 1991; 38: 984-993.

[3] Xiang YW, Hong YY, Yu Z, Zhong KF. Image denoising using SVM classification in non sub-sampled contourlet transform domain. Inform Sciences 2013; 246: 155-176.

[4] Cai N, Jian C, Jie Y. Applying a wavelet neural network to impulse noise removal. In: IEEE 2005 Neural Networks and Brain Conference; 13–15 October 2005; Media Center Hotel, Beijing, China. New York, NY, USA: IEEE. pp. 781-783.

[5] Vaseghi SV. Advanced Digital Signal Processing and Noise Reduction. 3rd ed. New York, NY, USA: Wiley, 2008.

[6] Singh KM, Bora PK, Singh SB. Rank-ordered mean filter for removal of impulse noise from images. In: IEEE 2002 Industrial Technology Conference; 11–14 December 2002; Bangkok, Thailand. New York, NY, USA: IEEE. pp. 980-985.

[7] Sedaaghi MH, Daj R, Khosravi M. Mediated morphological filters. In: IEEE 2001 Image Processing Conference; 7–10 October 2001; Thessaloniki, Greece. New York, NY, USA: IEEE. pp. 692-695.

[8] Wang Z, Zhang D. Progressive switching median filter for the removal of impulse noise from highly corrupted images. IEEE T Circuits-II 1999; 46: 78-80.

[9] Indu S, Chaveli R. A noise fading technique for images highly corrupted with impulse noise. In: IEEE 2007 Computing, Theory and Applications Conference; 5–7 March 2007; Kolkata, India. New York, NY, USA: IEEE. pp. 627-632.

[10] Nallaperumal K, Varghese J, Saudia S, Arilmozhi K, Velu K, Annam S. Salt & pepper impulse noise removal using adaptive switching median filter. In: IEEE 2006 Oceans Asia Pacific Conference; 16–19 May 2006; Singapore. New York, NY, USA: IEEE. pp. 1-8.

[11] How LE, Kai KM. Noise adaptive soft-switching median filter. IEEE T Image Process 2001; 10: 242-251.

[12] Fitri U, Keichii U, Gou K. High density impulse noise removal by fuzzy mean linear aliasing window kernel. In: IEEE 2012 Signal Processing, Communication and Computing Conference; 12–15 August 2012; Hong Kong. New York, NY, USA: IEEE. pp. 711-716.

[13] Song Y, Yunsang H, Sangkeun L. Pixel correlation-based impulse noise reduction. In: IEEE 2012 Frontiers of Computer Vision Conference; 9–11 February 2011; Ulsan, Korea. New York, NY, USA: IEEE. pp. 1-4.

[14] Zhang X, Youlun X. Impulse noise removal using directional difference based noise detector and adaptive weighted mean filter. IEEE Signal Proc Let 2009; 16: 295-298.

[15] Mu HH, Fan CC. Fast and efficient median filter for removing 1–99% levels of salt-and-pepper noise in images. Eng Appl Artif Intel 2013; 26: 1331-1338.

[16] Shi JH, Ling YH. Using sorted switching median filter to remove high-density impulse noises. J Vis Commun Image R 2013; 24: 956-967.

[17] Awad AS. Standard deviation for obtaining the optimal direction in the removal of impulse noise. IEEE Signal Proc Let 2011; 18: 407-410.

[18] Jafar I, Al Namneh R, Darabkh K. Efficient improvements on the BDND filtering algorithm for the removal of high density impulse noise. IEEE T Image Process 2013; 22: 1123-1232.

[19] Pei EN, Ma KK. A switching median filter with boundary discriminative noise detection for extremely corrupted images. IEEE T Image Process 2006; 15: 1506-1516.

[20] Wang W, Peizhong L. An efficient switching median filter based on local outlier factor. IEEE Signal Proc Let 2011; 18: 551-554.

[21] Xuming Z, Yi Z, Mingyue D, Wenguang H, Zhouping Y. Decision-based non-local means filter for removing impulse noise from digital images. Signal Process 2013; 93: 517–524.

[22] Jie SH. Adaptive salt-&-pepper noise removal: a function level evolution based approach. In: IEEE 2008 Adaptive Hardware and Systems Conference; 22–25 June 2008; Noordwijk, Netherlands. New York, NY, USA: IEEE. pp. 391-397.

[23] Wang Z, David Z. Restoration of impulse noise corrupted images using long-range correlation. IEEE Signal Proc Let 1998; 5: 4-7.

[24] Markus MB, Hans PK, Raymond T, Sander NJ. LOF: identifying density-based local outliers. ACM 2000 Sigmod Record Conference; 16–18 May 2000; New York, NY, USA: ACM. pp. 93-104.

[25] Varghese J, Mohamed G, Saudia S, Madappa S, Mohamed SK, Omer BH. An efficient adaptive fuzzy based switching weighted average filter for the restoration of impulse corrupted digital images. IET Image Process 2014; 8: 199-206.

[26] Hwang H, Haddad R. Adaptive median filters: new algorithms and results IEEE T Image Process 1995; 4: 499-502.